ACS OMEGA

Open Access

http://pubs.acs.org/journal/acsodf

Article

$K_6[P_2Mo_{18}O_{62}]$ as DNase-Mimetic Artificial Nucleases to Promote Extracellular Deoxyribonucleic Acid Degradation in Bacterial Biofilms

Shaoling Lin, Jing Li, Feng Zhou, Bee K. Tan, Baodong Zheng,* and Jiamiao Hu*

Cite This: *ACS Omega* 2023, 8, 33966−33974

Read Online

ACCESS | Metrics & More | Article Recommendations

ABSTRACT: In the current study, the DNase-like activity of the Dawson-type polyoxometalate $K_6[P_2Mo_{18}O_{62}]$ was explored. The obtained findings demonstrated that $K_6[P_2Mo_{18}O_{62}]$ could effectively cleave phosphoester bonds in the DNA model substrate (4-nitrophenyl phosphate) and result in the degradation of plasmid DNA. Moreover, the application potential of this Dawson-type polyoxometalate as a DNase-mimetic artificial enzyme to degrade extracellular DNA (eDNA) in *Escherichia coli* (*E. coli*) bacterial biofilm was explored. The results demonstrated that $K_6[P_2Mo_{18}O_{62}]$ exhibited high cleavage ability toward eDNA secreted by *E. coli* and thus eradicated the bacterial biofilm. In conclusion, Dawson-type polyoxometalate $K_6[P_2Mo_{18}O_{62}]$ possessed desirable DNase-like activity, which could serve as a bacterial biofilm eradication agent by cleaving and degrading eDNA molecules.

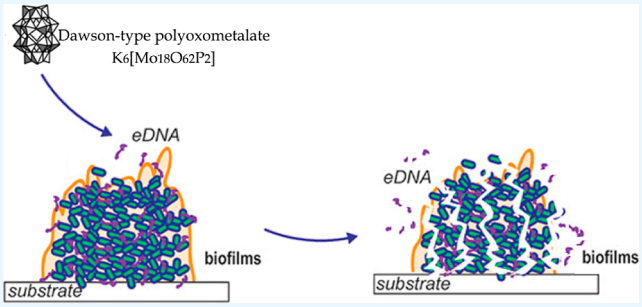

1. INTRODUCTION

Polyoxometalates (POMs) are a diverse group of metal−oxygen clusters formed by oxygen bonding of transition-metal ions (such as Mo, W, V, Nb, etc.),[1] which have been discovered over the past 200 years.[2] To date, 10 basic topology structures of POMs (Keggin, Dawson, Silverton, Anderson, Waugh, Lindqvist, Weakley, Standberg, Finke, and Preyssler) have been discovered,[3] with Keggin and Dawson structures being most extensively studied.[4−6] Recently, emerging multidisciplinary research in POM chemistry further revealed a series of POM clusters with novel topologies and high-dimensional extended architectures, such as lanthanide-functionalized POMs,[7−9] POM-based supramolecular frameworks,[10] POM-based inorganic−organic hybrids,[11−14] etc.

In the past two decades, research progress in POM chemistry has unraveled the great potential of POMs in many useful applications, such as chemical catalysis,[15,16] electrochemical sensors,[17] pharmaceutical analysis,[18,19] protein crystallization,[20] antitumor therapy,[21,22] and antimicrobial treatment,[23,24] etc. Besides, it is also worth mentioning that several Dawson-type POMs (e.g., $H_6[Mo_{18}O_{62}P_2]$, etc.) have been reported as tyrosinase inhibitors and used for mushroom preservation, showing the great potential of POMs for food preservation.[25,26] Moreover, recent studies have further noted that the POMs could function as artificial nucleases. Particularly, the nuclease-like activity of Keggin-type POMs has already been well illustrated. For instance, Luong et al. reported that the Keggin-type POM $[(a\text{-}PW_{11}O_{39}Zr(\mu\text{-}OH)(H_2O))_2]^{8-}$ (ZrK 2:2) could cleave the supercoiled plasmid into the linear form.[27] The Keggin-type POM with a similar structure $(Et_2NH_2)_8[(\alpha\text{-}PW_{11}O_{39}Zr(\mu\text{-}OH)(H_2O))_2]\cdot 7H_2O$ (ZrK 2:2) was also found to hydrolyze the ester bond of 2-hydroxypropyl-4-nitrophenyl phosphate (HPNP, a model RNA substrate).[28] However, to the best of our knowledge, there is still a lack of knowledge about the nuclease activity of other types of POMs, though evidence suggests several Well-Dawson POMs ($Zr[\alpha_2\text{-}P_2W_{17}]_2$, $Hf[\alpha_2\text{-}P_2W_{17}]_2$), ($[Zr_4(P_2W_{16}O_{59})_2(\mu_3\text{-}O)_2(OH)_2(H_2O)_4]^{14-}$) may catalytically hydrolyze phosphoester bonds in DNA model substrates [4-nitrophenyl phosphate (NPP) and bis-4-nitrophenyl phosphate (BNPP)][29,30] and RNA model substrate (HPNP).[29] However, their nuclease-like activity has not yet been confirmed in DNA molecules. Therefore, in the current study, a Dawson-type POM $K_6[P_2Mo_{18}O_{62}]$ was synthesized, and its nuclease-like activity was first determined using both the DNA model substrate (4-nitrophenyl phosphate) and plasmid DNA.

Moreover, the application of a DNase-like compound to degrade extracellular DNA (a kind of nucleic acid existing in bacterial extracellular biofilm) has been proposed as an effective

Received: July 5, 2023
Accepted: August 25, 2023
Published: September 4, 2023

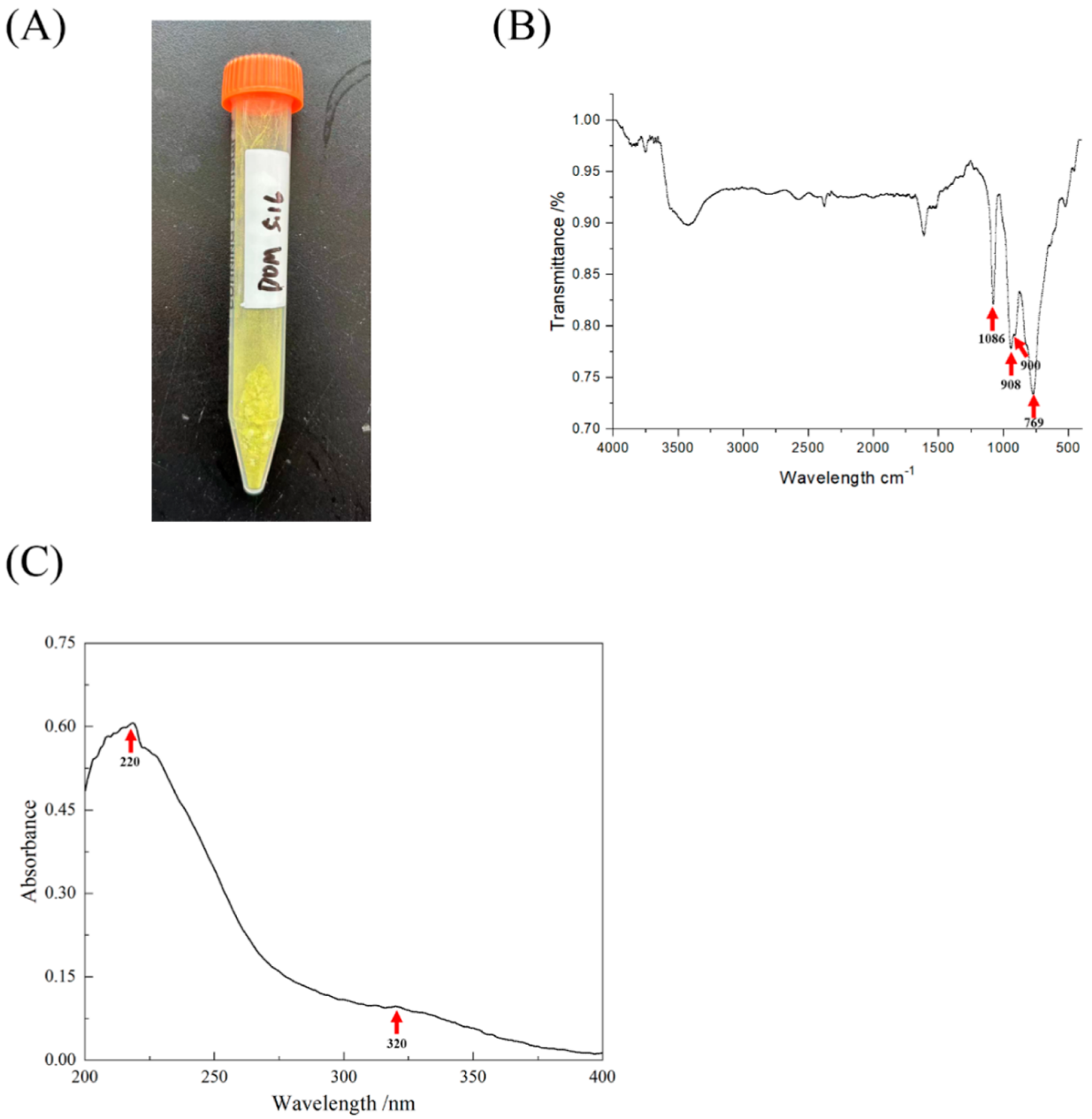

Figure 1. Synthesis and characterization of Dawson-type POM $K_6[P_2Mo_{18}O_{62}]$. (A) Picture of as-synthesized $K_6[P_2Mo_{18}O_{62}]$; (B) Fourier transform infrared spectra; and (C) UV−visible spectra of as-synthesized $K_6[P_2Mo_{18}O_{62}]$.

strategy to prevent, disperse, or sensitize bacterial biofilm. For instance, Yu et al. showed that DNase I, but not protease, could break down the microbial biofilm.[31] Panariello et al. also reported that DNase I significantly reduced eDNA in *Candida albicans* biofilms.[32] However, the relatively high price and low stability greatly limited the practical potential of DNase I in eradicating bacterial biofilm.[33,34] Therefore, the potential application of this Dawson-type POM as a bacterial biofilm eradication agent was also tested in the current study.

2. MATERIALS AND METHODS

2.1. Materials. Sodium molybdate dihydrate (99%), phosphoric acid (85%), hydrochloric acid (SCR, 36−38%), potassium bromide (90%), and 4-nitrophenyl phosphate disodium salt hexahydrate (NPP, 99%) were purchased from Macklin. *Escherichia coli* (*E. coli*) O157/H7 was purchased from the China Industrial Culture Collection.

2.2. Synthesis and Characterization of Dawson-Type Polyoxometalate $K_6[P_2Mo_{18}O_{62}]$. The Dawson-type POM $K_6[P_2Mo_{18}O_{62}]$ was prepared according to Hu et al.[35] In brief, 40 g of sodium molybdate dihydrate, 6 mL of phosphoric acid, and 33 mL of hydrochloric acid were heated at reflux in 100 mL of purified water for 8 h. Then, 40 g of potassium bromide was mixed in a solution cooled to room temperature and left overnight at 4 °C to recrystallize. The solids collected through vacuum filtration were then dissolved in 100 mL of purified water to remove impurities. Recrystallization was repeated three times to ensure the high purity of the compound. Finally, the yellow compound obtained through filtration, named Dawson POM $K_6[P_2Mo_{18}O_{62}]$, was dried at room temperature for later use.

https://doi.org/10.1021/acsomega.3c04790
ACS Omega 2023, 8, 33966−33974

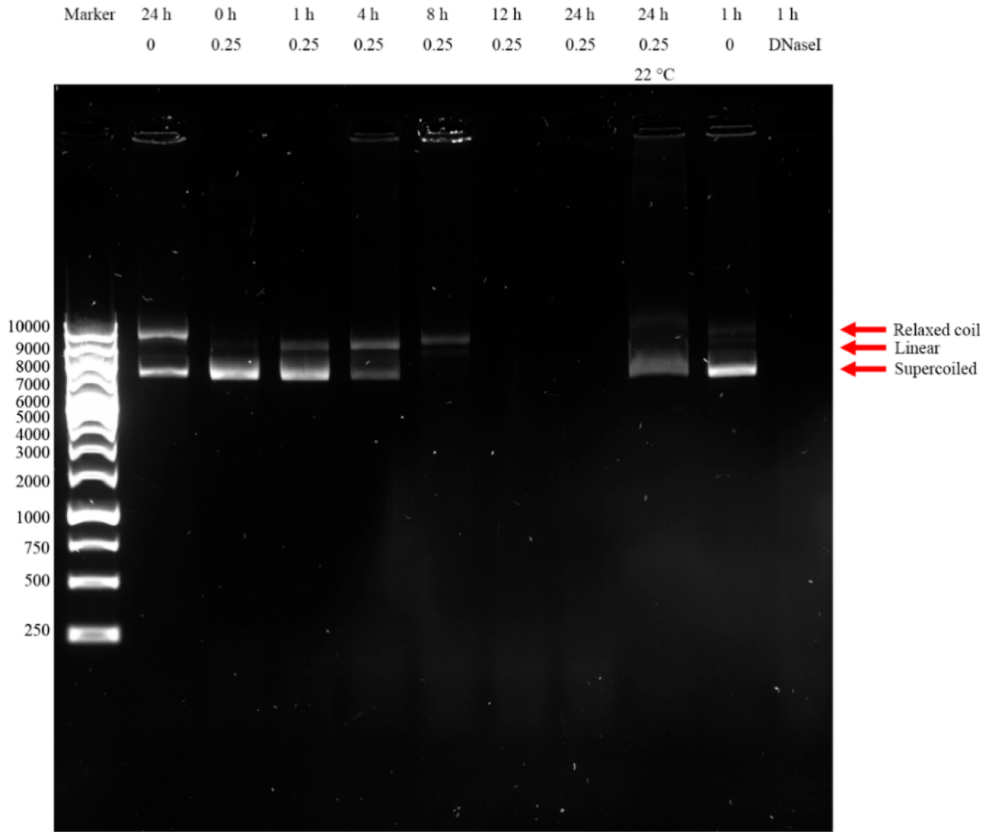

Figure 2. Complete degradation of the plasmid by Dawson-type POM $K_6[P_2Mo_{18}O_{62}]$. Lane 1 DL15,000 DNA marker. Lane 2 plasmid DNA was incubated at 37 °C. Lane 3−8 plasmid DNA was incubated with 0.25 mM $K_6[P_2Mo_{18}O_{62}]$ at 37 °C for 0−24 h. Lane 9 plasmid DNA was incubated with 0.25 mM $K_6[P_2Mo_{18}O_{62}]$ at 22 °C for 0−24 h. Lane 10−11 plasmid DNA was treated without or with DNase I for 1 h.

Infrared spectra of $K_6[P_2Mo_{18}O_{62}]$ (4000−500 cm^{-1}) were recorded using a Tensorii Fourier transform infrared spectrometer (Bruker, Billerica MA, USA). The UV spectrum was measured by a NanoDrop 2000 spectrophotometer (Thermo Scientific, Waltham, MA, USA) in the range of 200−400 nm when the concentration of $K_6[P_2Mo_{18}O_{62}]$ was 0.15 mg/mL.

2.3. Plasmid DNA and Genomic DNA Degradation Assay. Plasmid DNA and genomic DNA were extracted by the E.Z.N.A. plasmid DNA mini kit I or E.Z.N.A. Bacterial DNA kit (omega) from *E. coli*. Subsequently, plasmid DNA or genomic DNA solution and $K_6[P_2Mo_{18}O_{62}]$ solution were mixed and incubated for different periods of time before agarose gel electrophoresis was performed to detect DNA breakage.

2.4. Fluorescence Quenching Assay. According to the method of Lu et al.,[36] 10 mg of calf thymus DNA (ctDNA) was dissolved in 10 mL of sterile enzyme-free water, and 1 μL GelRed nucleic acid dye was added to obtain a GelRed−DNA mixture. Then, 100 μL of GelRed−DNA mixture and 100 μL of $K_6[P_2Mo_{18}O_{62}]$ solution (at different concentrations) were mixed in a 96-well black base plate. After incubation for 10 min, the fluorescence spectra at an emission wavelength of 540−800 nm were determined by a multimode microplate reader (Molecular Devices, U.S.A).

2.5. NMR Spectroscopy. The experiment was carried out as reported by Vanhaecht et al.[30] Sterile and enzyme-free water was precisely configured with a 20 mM $K_6[P_2Mo_{18}O_{62}]$ solution and DNA simulant 4-nitrophenyl phosphate disodium salt hexahydrate solution (NPP), and the two liquids were evenly mixed by equal volume. Subsequently, the pH of the mixed solution was adjusted to 6.79. After incubation at 37 °C for different times, the NMR spectra of the mixed liquid were determined by an AVANCE Neo 600 m full digital NMR spectrometer (Bruker, Billerica, MA, USA).

2.6. Quantification of Biofilm Production by a Microtiter Plate Assay. *E. coli* was cultured in 200 μL of LB liquid medium in a 96-well plate at 37 °C for 2 days without shaking. Then, the plates were rinsed slowly with PBS three times to remove floating bacteria. Next, 200 μL of $K_6[P_2Mo_{18}O_{62}]$ solution was added to the plate and incubated at 37 °C for 4 h. DNase I solution was used as the positive control. Then, the plates were rinsed slowly with PBS before a crystal violet (1%) aqueous solution was added to stain the bacteria for 15 min. Finally, after rinsing with PBS again, 200 μL of anhydrous ethanol was added, and the optical density was determined at 570 nm.

2.7. Confocal Laser Scanning Microscopy. *E. coli* was cultured in LB liquid medium in a 6-well plate containing cell slides (diameter: 9 mm) and cultured at 37 °C for 2 days. Two days later, the cell slides were removed and slowly rinsed with PBS three times to remove the floating bacteria on the cell slides. Then, the slides were placed in $K_6[P_2Mo_{18}O_{62}]$ solutions of different concentrations, and DNase I was used as the positive control. After incubation at 37 °C for 4 h, the biofilm-coated cell sliders were slowly rinsed with PBS three times and fixed with 2.5% glutaraldehyde for 30 min. Then, the cells were stained with 0.01% acridine orange (W/V) under dark conditions for 15 min. Finally, after washing PBS, confocal laser scanning microscopy was used for the observation of biofilm. The observation conditions were an emission wavelength of 525 nm and an excitation wavelength of 488 nm. The three-dimensional

https://doi.org/10.1021/acsomega.3c04790
ACS Omega 2023, 8, 33966−33974

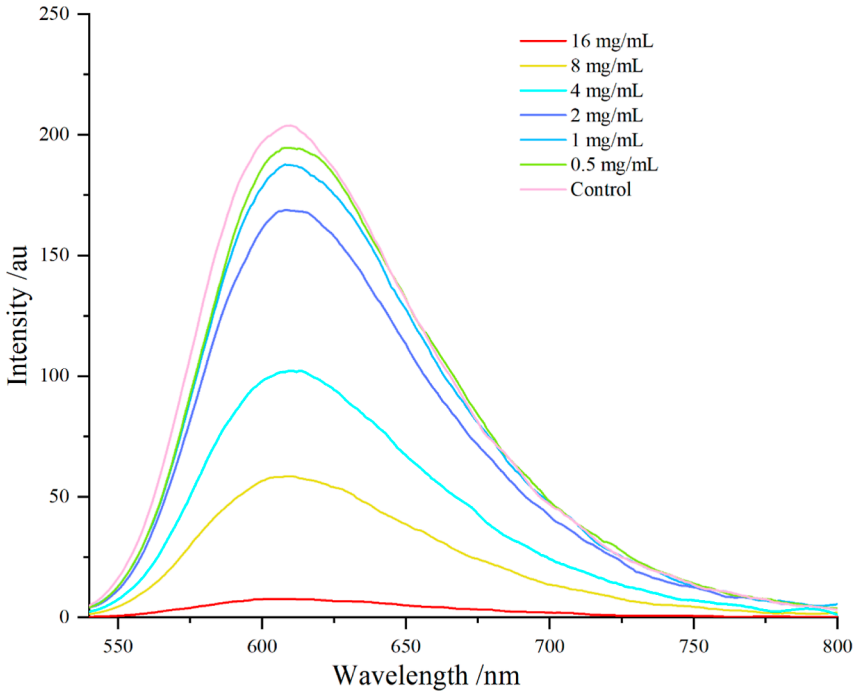

Figure 3. Fluorescence spectra of GelRed−ctDNA quenched by Dawson-type POM $K_6[P_2Mo_{18}O_{62}]$. The ctDNA and GelRed nucleic acid dye mixtures were incubated with $K_6[P_2Mo_{18}O_{62}]$ (at different concentrations). The fluorescence spectra at an emission wavelength of 540−800 nm were determined by a multimode microplate reader.

structure of the biofilm was mapped using a ZEN Lite 2012 (Car Zeiss Microscopy GmbH, Germany).

2.8. Quantification of Biofilm eDNA. The eDNA in biofilm was quantified according to previous literature.[37] In brief, biofilms were grown in LB liquid medium in a 96-well plate at 37 °C for 2 days without shaking before being incubated with $K_6[P_2Mo_{18}O_{62}]$ for 4 h. After the medium was carefully removed and the biofilm of each well was properly disintegrated and dissolved in 200 μL of H_2O by agitation for 5 min. After centrifugation at 8000*g* for 10 min, the supernatant was collected. The supernatant was transferred to a tube, and eDNA was further extracted using phenol/chloroform/isoamyl alcohol (25:24:1) extraction and ethanol precipitation. The obtained eDNA was then quantified by real-time PCR according to the previous literature[38] using SYBR Green Master Mix and primers targeting the reference gene *purA* (*purA*-F: 5′-GGGCCTGCTTATGAAGATAAAGT-3′; *purA*-R: 5′-TCAACCACCATAGAAGTCAGGAT-3′). Purified *E. coli* genomic DNA at known concentrations was subjected to real-time PCR to generate a standard curve used to normalize the concentration of eDNA in the unknown samples.

2.9. Statistical Analysis. All experimental measurements were conducted at least in triplicate, and the reported data points are expressed as the mean ± standard deviation where feasible. Origin 2021 was used to analyze the data and prepare the figures. A *p*-value of less than 0.05 was reported as statistically significant.

3. RESULTS

3.1. Synthesis and Characterization of Dawson Polyoxometalate $K_6[P_2Mo_{18}O_{62}]$. The Dawson POM $K_6[P_2Mo_{18}O_{62}]$ was synthesized according to a previous report. The obtained powder showed a light-yellow color (Figure 1A), which was subsequently characterized by infrared spectra. The results showed the characteristic peaks of $[P_2Mo_{18}O_{62}]$ at 769, 900, 908, and 1086 cm^{-1} (representing the stretching vibration characteristic peaks of Mo−O_c−Mo, Mo−O_b−Mo, Mo−O_d, and P−O_a, respectively) (Figure 1B). The UV spectra also showed a strong absorption peak appearing at 220 nm, which can be attributed to the charge transfer transition of O_d−Mo, while another weak peak at 320 nm might belong to the charge transfer transition of O_{b+c}−Mo (Figure 1C). Indeed, the obtained infrared spectra and UV spectra were consistent with the IR and UV properties of POM $H_6[P_2Mo_{18}O_{62}]$ reported previously.[39] Taken together, the results showed that the Dawson POM $K_6[P_2Mo_{18}O_{62}]$ was successfully synthesized.

3.2. Plasmid DNA Degradation in the Presence of Dawson Polyoxometalate $K_6[P_2Mo_{18}O_{62}]$. To determine the potential nuclease-like activity of $K_6[P_2Mo_{18}O_{62}]$, the cleavage and fragmentation of plasmid DNA induced by $K_6[P_2Mo_{18}O_{62}]$ were visualized by agarose gel electrophoresis. As shown in Figure 2, upon incubation with $K_6[P_2Mo_{18}O_{62}]$, the supercoiled plasmid DNA could be cut into a linear form quickly, which was the same as the action of Keggin-type POM. Interestingly, further incubation (>8 h) with $K_6[P_2Mo_{18}O_{62}]$ resulted in the plasmid DNA becoming smeared, and a longer incubation period resulted in more obvious degradation of the plasmid DNA fragmentation, which is similar to the phosphatase activity of DNase I. Interestingly, in the previous report, incubation of plasmid DNA with Keggin-type POM up to 46 h only resulted in the formation of linear plasmid DNA,[27] indicating these two types of POMs might both cleave plasmid DNA but in different ways. In addition, we also tested the nuclease activity of $K_6[P_2Mo_{18}O_{62}]$ against plasmid DNA at room temperature (22 °C). The result demonstrated that $K_6[P_2Mo_{18}O_{62}]$ could also effectively degrade plasmid DNA, though the reaction became slower due to the decrease in temperature.

3.3. Fluorescence Quenching Analysis of the Interaction between $K_6[P_2Mo_{18}O_{62}]$ and DNA. The artificial

https://doi.org/10.1021/acsomega.3c04790
ACS Omega 2023, 8, 33966−33974

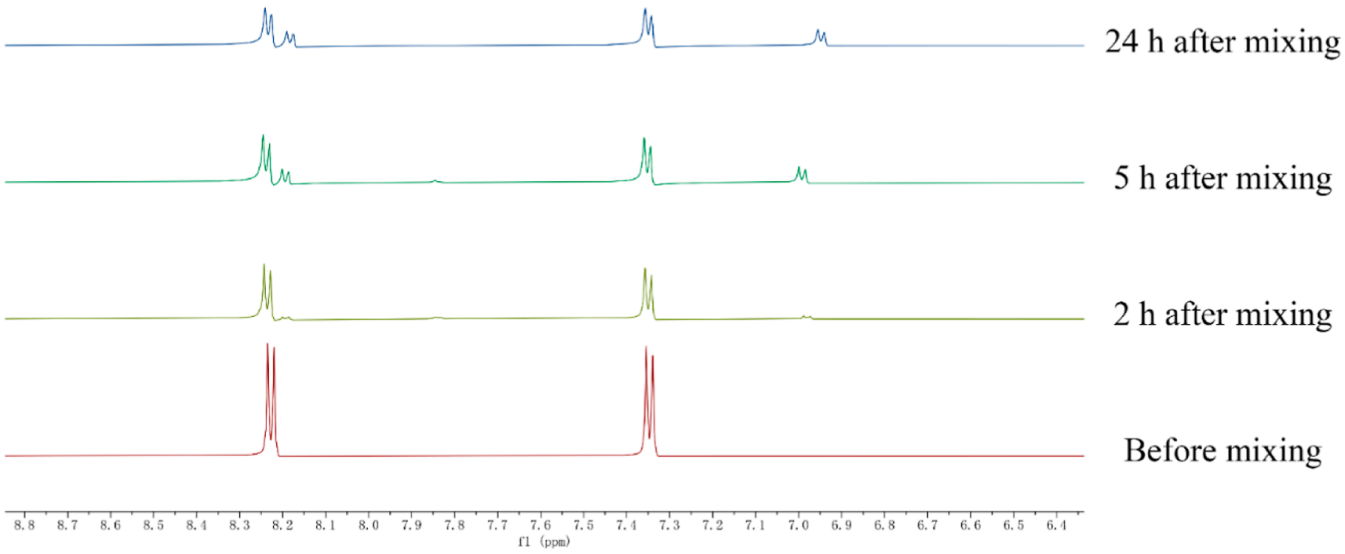

Figure 4. ^{1}H NMR−NMR spectra of the DNA model substrate (NPP) incubated with Dawson-type POM $K_6[P_2Mo_{18}O_{62}]$ in different time intervals. $K_6[P_2Mo_{18}O_{62}]$ and DNA simulant 4-nitrophenyl phosphate disodium salt hexahydrate solution (NPP) were evenly mixed and incubated at 37 °C at different times. The NMR spectra of the mixed liquid were determined by an AVANCE Neo 600 m full digital NMR spectrometer.

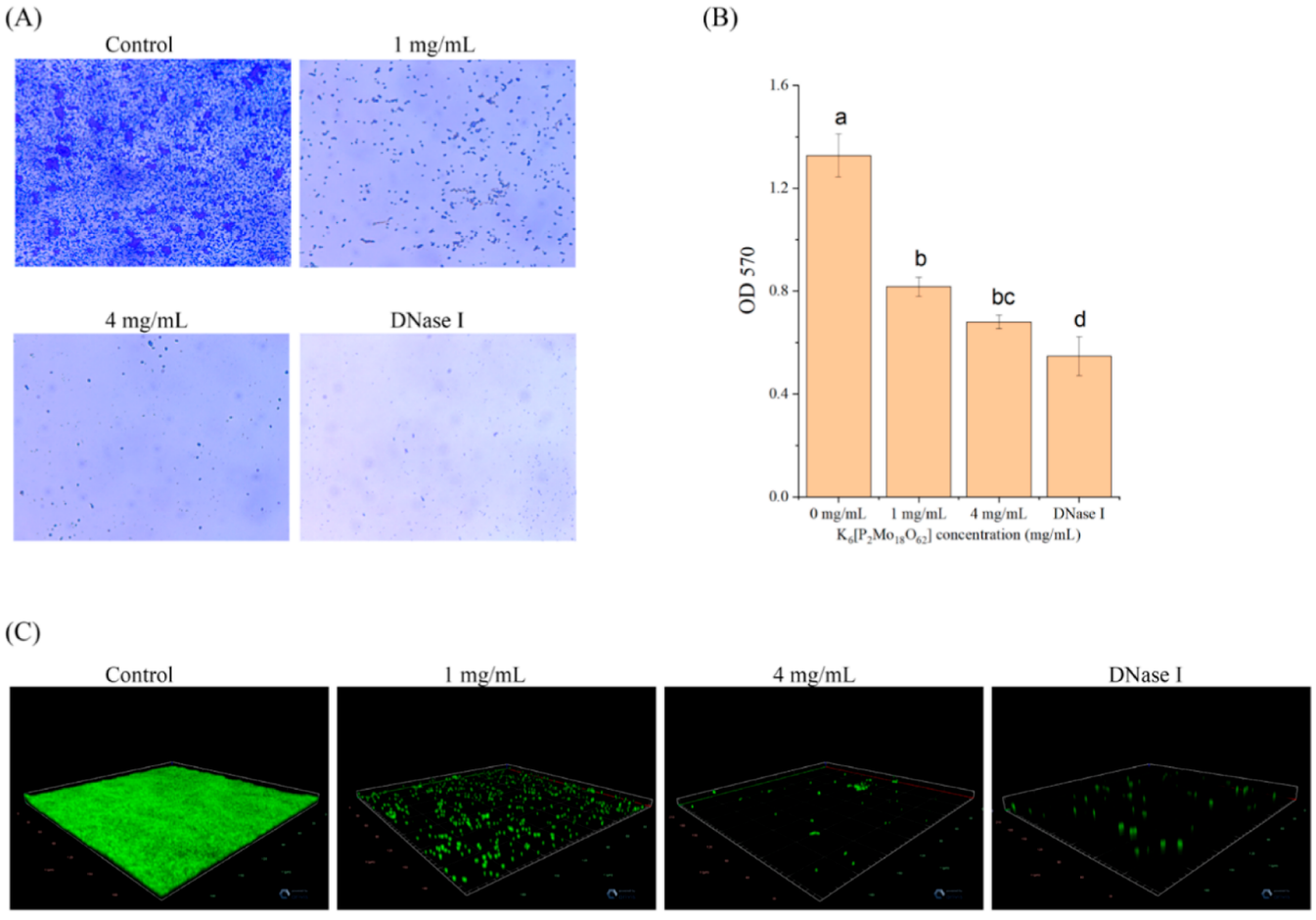

Figure 5. Eradicating effect of Dawson-type POM $K_6[P_2Mo_{18}O_{62}]$ on the *E. coli* biofilm. (A) Eradicating effect of $K_6[P_2Mo_{18}O_{62}]$ on the biofilm observed by crystal violet staining; (B) biofilm quantification ($OD_{570\ nm}$) of above crystal staining; (C) eradicating effect of $K_6[P_2Mo_{18}O_{62}]$ on biofilm observed by confocal laser scanning microscopy. Different lowercase letters represent significant differences ($p < 0.05$).

nucleases often possess the ability to interact with DNA and thus quench the DNA fluorescent probe.[40] Here, we also tested the quenching effects of $K_6[P_2Mo_{18}O_{62}]$ on GelRed nucleic acid dye with ctDNA. As shown in Figure 3, the excited fluorescence intensity of the GelRed−DNA complex at 610 nm decreased gradually upon the addition of $K_6[P_2Mo_{18}O_{62}]$ with a dose-

https://doi.org/10.1021/acsomega.3c04790
ACS Omega 2023, 8, 33966−33974

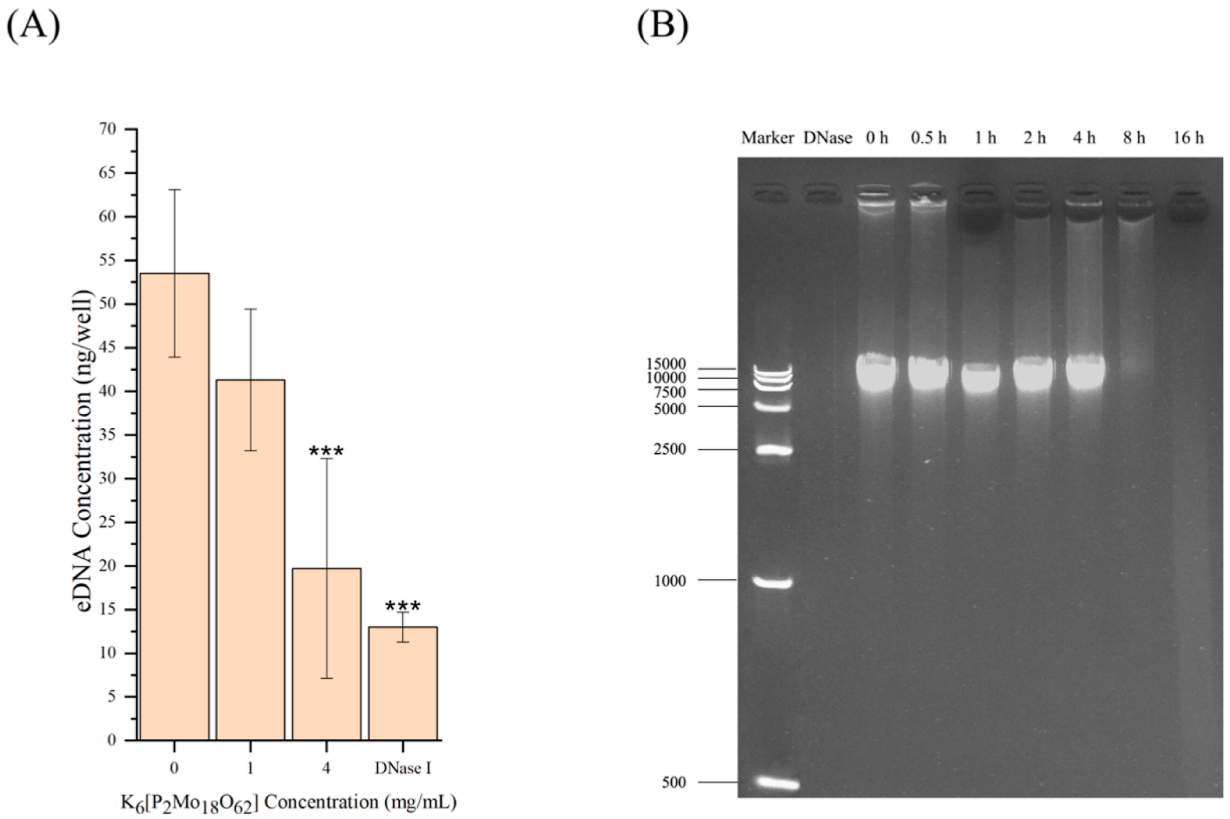

Figure 6. Catalytic activity of $K_6[P_2Mo_{18}O_{62}]$ in the hydrolysis of eDNA in the biofilm. (A) Quantification of eDNA in unwashed *E. coli* biofilms present in 96-well plates. The experimental wells with *E. coli* biofilms were loaded with $K_6[P_2Mo_{18}O_{62}]$ or DNase I. The total eDNA in each well was quantified by real-time PCR using primers specific for *purA*. (***$p < 0.001$). (B) Cleavage of genomic DNA of *Escherichia coli* catalyzed by $K_6[P_2Mo_{18}O_{62}]$. Lane 1 DL15,000 DNA marker. Lane 2 genomic DNA incubated with DNase I at 37 °C for 16 h. Lane 3−9 genomic DNA was incubated with 4 mg/mL $K_6[P_2Mo_{18}O_{62}]$ at 37 °C for 0−16 h.

dependent trend, indicating that the POM $K_6[P_2Mo_{18}O_{62}]$ might competitively bind to ctDNA, resulting in less interaction between GelRed nucleic acid dye and ctDNA.

3.4. Hydrolysis of DNA Analogue 4-Nitrophenylphosphate Disodium (NPP) by $K_6[P_2Mo_{18}O_{62}]$. To further confirm the phosphatase activity of $K_6[P_2Mo_{18}O_{62}]$, we also determined the hydrolysis of NPP (a DNA mimic commonly used as a model substrate to present the phosphate bond in DNA[41]) in the presence of $K_6[P_2Mo_{18}O_{62}]$. The NMR analysis was performed to monitor the hydrolytic reaction of NPP (2.0 mM) with $K_6[P_2Mo_{18}O_{62}]$ (2.0 mM) at different time intervals.

As can be seen from Figure 4, The ^{1}H NMR spectra showed that in the course of the hydrolytic reaction, the resonances of the *ortho*-protons of NPP (7.34 and 8.22 ppm) gradually weakened, and new resonances (6.89 and 8.18 ppm) appeared, unambiguously attributed to the *ortho*-protons of *p*-nitrophenol (NP).[28] Meanwhile, with the increase in reaction time, the NP formant gradually shifted to the right, which is a high-field displacement caused by the hydroxyl group in NPP rather than the presence of a phosphate group.[30] Therefore, the experimental results also confirmed that $K_6[P_2Mo_{18}O_{62}]$ possesses phosphatase activity and can hydrolyze the phosphate ester bonds in the DNA analogue NPP to form NP.

3.5. Eradicating Effect of $K_6[P_2Mo_{18}O_{62}]$ on the *E. coli* Biofilm. To further explore the potential uses of the artificial nuclease activity of $K_6[P_2Mo_{18}O_{62}]$, we further explored its scavenging potential for *E. coli* biofilms. Crystal violet staining and three-dimensional confocal laser scanning microscopy were used to analyze the antibiofilm efficacy of $K_6[P_2Mo_{18}O_{62}]$. As can be seen from Figure 5A, an obvious biofilm was formed in the control group after incubation for 48 h at 37 °C. However, both DNase I and $K_6[P_2Mo_{18}O_{62}]$ treatments effectively eradicated the biofilm formation. The quantitative measurements of the absorbance value at 570 nm also supported this finding that less crystal violet stuck to the biofilm in the bacteria treated with DNase I and $K_6[P_2Mo_{18}O_{62}]$ (Figure 5B).

The three-dimensional confocal laser scanning microscopy also revealed that the $K_6[P_2Mo_{18}O_{62}]$ treatment changed the thickness and surface morphology of the *E. coli* biofilm (Figure 5C). The overall structure of the biofilm in the control group was dense and thick, with a slightly uneven surface but no holes. However, the biofilms treated by DNase I and $K_6[P_2Mo_{18}O_{62}]$ showed a thinner biofilm structure, with large areas of "holes" sparsely appearing on the biofilm. These results indicated that $K_6[P_2Mo_{18}O_{62}]$ treatment could greatly disrupt the integrity of the *E. coli* biofilm.

3.6. Cleavage of *E. coli* Biofilm eDNA by $K_6[P_2Mo_{18}O_{62}]$. To better understand the association between the nuclease activity of $K_6[P_2Mo_{18}O_{62}]$ and its antibiofilm activity, the changes in eDNA amount present in each well of biofilms upon $K_6[P_2Mo_{18}O_{62}]$ treatment were determined by real-time PCR. As shown in Figure 6, using *purA* as a reference gene, the average amounts of eDNA in $K_6[P_2Mo_{18}O_{62}]$ (@4 mg/mL)-treated and DNase I-treated wells were significantly reduced by factors of about 3 and 4, respectively, compared with the untreated control biofilm (Figure 6A), suggesting that $K_6[P_2Mo_{18}O_{62}]$-disrupted bacterial biofilm could be attributed, at least partially, to its eDNA cleavage activity. In addition, as previous studies showed

https://doi.org/10.1021/acsomega.3c04790
ACS Omega 2023, 8, 33966−33974

that the eDNA in biofilms is similar to the bacterial genome DNA,[42,43] the genomic DNA of *E. coli* was extracted and used as the substrate to confirm the catalytic activity of $K_6[P_2Mo_{18}O_{62}]$ in the hydrolysis of eDNA. As can be seen from Figure 6B, $K_6[P_2Mo_{18}O_{62}]$ effectively cleaved genomic DNA, suggesting that $K_6[P_2Mo_{18}O_{62}]$ could promote the hydrolysis of natural DNAs, such as eDNA in the biofilm.

4. DISCUSSION

POMs represent a large class of polynuclear metal-oxo clusters with a wide variety of physical and chemical properties. Since its discovery in the 1700s, POM-related research has attracted increasing attention from scholars in different disciplines. To date, POMs are of interest in the fields of chemistry such as chemical catalysis,[44] electronics, electronic sensors,[45] physics, magnetic materials,[46] biomedicine, antitumor, antivirus, antibacterial, antidiabetic,[47] etc.

In the past decades, the range of POM activities has been continuously expanded. In particular, several studies have reported that the POMs possess DNA-cleaving activity. For example, dimeric tetrazirconium(IV) Wells−Dawson POM $[(a\text{-}PW_{11}O_{39}Zr(\mu\text{-}OH)(H_2O))_2]^{8-}$ (ZrK 2:2) was found to be active toward hydrolysis of both DNA and RNA model substrates. Particularly, the zirconium ion at the α2-position was identified as the active site for the hydrolysis.[29] Notably, in another study reported by the same group, the potential phosphatase activity of several metal-substituted Wells−Dawson POMs (with the same structure but different metal substitutions) was compared using the DNA model substrates BNPP and NPP. The results also showed that the metal ion at the α2-position was the determining factor for the phosphatase activity of the POMs.[30] Here, our study also revealed that Dawson-type POM $K_6[P_2Mo_{18}O_{62}]$ could result in complete degradation of plasmid DNA, which is unique to the action of Keggin-type POM $[(a\text{-}PW_{11}O_{39}Zr(\mu\text{-}OH)(H_2O))_2]^{8-}$ (ZrK 2:2) reported previously.[27] The structure difference between Keggin-type and Wells−Dawson-type POMs (e.g., Wells−Dawson sandwich-type POMs consist of two incomplete Keggin sets) may contribute to the observed distinct DNA-cutting patterns. Meanwhile, the molybdenum ions (instead of zirconium ions) at the α2-position in $K_6[P_2Mo_{18}O_{62}]$ might be another cause to promote the complete degradation of plasmid DNA. However, further studies are needed to confirm these hypotheses and explore the potential phosphatase activity of other types of POMs (e.g., lacunary POMs or mixed metal POMs).

Additionally, the results obtained from the fluorescence quenching assay and NMR spectroscopy also supported the above findings. Here, $K_6[P_2Mo_{18}O_{62}]$ was found to reduce the fluorescence intensity of the GelRed−ctDNA complex, suggesting a potential competitive binding of $K_6[P_2Mo_{18}O_{62}]$ to the ctDNA. A similar observation was also reported for other compounds with artificial nuclease activity. For example, Steiner et al. showed that the artificial nuclease Cu(II) benzothiazole complex could replace ethidium bromide and embed in DNA competitively.[48] The NMR spectroscopy also revealed that the phosphoester hydrolysis of DNA mimics NPP into NP and could occur in the presence of $K_6[P_2Mo_{18}O_{62}]$. Indeed, NPP hydrolysis has been widely used to characterize the activity of artificial nucleases such as cyclen-based artificial nucleases,[49] Zinc(II) complex with histidine-containing pseudopeptide[50] as well as $Na_{14}[Zr_4(P_2W_{16}O_{59})_2(\mu_3\text{-}O)_2(OH)_2(H_2O)_4]\cdot 57H_2O$ (ZrWD 4:2).[29]

Bacteria do not always exist as dispersed single cells but could also form structured surface-attached communities known as biofilms, which pose a great threat to the health and food industries. The bacteria in the biofilm are embedded in an extracellular matrix, which plays key roles in regulating the biofilm lifestyle and virulence. Indeed, the extracellular matrix could account for over 90% of the biofilm dry mass, which is composed of extracellular polysaccharides, eDNA, and proteins. Since extracellular polysaccharides are considered as the major structural components of the biofilm matrix, dispersion of extracellular polysaccharide substances has become a promising strategy to combat the biofilm.[51] Recently, the pivotal role of eDNA in maintaining biofilm structural integrity has also been well recognized.[52,53] Therefore, a number of studies have revealed that nuclease DNase I could effectively disrupt the biofilm of various bacteria, such as *E. coli*,[54] *Pseudomonas aeruginosa*,[55] *Enterococcus faecalis*,[56] *Staphylococcus aureus*,[57] *Listeria monocytogenes*,[58] and *Vibrio parahemolyticus*.[59]

However, high costs and low stability greatly limited the practicality of DNase I as an antibiofilm agent in practice.[60] Indeed, the search for low-cost, stable, and easy-to-synthesize DNase-mimetic artificial enzymes as antibiofilm agents has drawn great attention in the past decades.[61] Here, as demonstrated above, the Dawson-type POM $K_6[P_2Mo_{18}O_{62}]$ could effectively remove mature *E. coli* biofilms and significantly destroy the structure of the biofilm. Meanwhile, quantification of eDNA by real-time PCR also showed that $K_6[P_2Mo_{18}O_{62}]$ significantly reduced the content of eDNA in mature biofilms. It is worth mentioning that the raw materials for $K_6[P_2Mo_{18}O_{62}]$ synthesis are low-cost and the synthesis process has been well-established;[62,63] therefore, these advantages will make this Dawson-type POM a cost-effective antibiofilm agent with huge potential for practical application.

5. CONCLUSIONS

In the current study, a Dawson-type POM $K_6[P_2Mo_{18}O_{62}]$ was synthesized according to the literature, which possesses good phosphatase activity and could degrade plasmid DNA in vitro. Furthermore, this Dawson-type POM showed desirable scavenging activity on the *E. coli* biofilm with the ability to reduce the level of eDNA. In conclusion, the Dawson-type POM $K_6[P_2Mo_{18}O_{62}]$ could serve as a promising biofilm-degrading artificial nuclease.

■ ASSOCIATED CONTENT

Data Availability Statement

The data used to support the findings of this study are included in the article.

■ AUTHOR INFORMATION

Corresponding Authors

Baodong Zheng − *College of Food Science, Fujian Agriculture and Forestry University, Fuzhou 350002, China;* orcid.org/0000-0003-3133-1219; Email: zbdfst@163.com

Jiamiao Hu − *College of Food Science, Fujian Agriculture and Forestry University, Fuzhou 350002, China; College of Life Sciences, University of Leicester, Leicester LE1 7RH, U.K.;* orcid.org/0000-0001-6489-9877; Email: jiamiao.hu@fafu.edu.cn

https://doi.org/10.1021/acsomega.3c04790
ACS Omega 2023, 8, 33966−33974

Authors

Shaoling Lin − *College of Food Science, Fujian Agriculture and Forestry University, Fuzhou 350002, China;* orcid.org/0000-0001-7631-1006

Jing Li − *College of Food Science, Fujian Agriculture and Forestry University, Fuzhou 350002, China*

Feng Zhou − *College of Food Science, Fujian Agriculture and Forestry University, Fuzhou 350002, China*

Bee K. Tan − *College of Life Sciences, University of Leicester, Leicester LE1 7RH, U.K.*

Complete contact information is available at: https://pubs.acs.org/10.1021/acsomega.3c04790

Author Contributions

S.L. and J.L. contributed equally to this work. S.L.: conceptualization and funding acquisition; writing—original draft; J.L.: investigation, formal analysis, and visualization; F.Z.: investigation; B.K.T.: writing—review and editing; B.Z.: supervision; J.H.: conceptualization and funding acquisition; writing—review and editing; all the authors made substantial contributions to the study. All authors have seen, approved, and are fully conversant with the contents of the manuscript.

Notes

The authors declare no competing financial interest.

■ ACKNOWLEDGMENTS

The authors appreciate the financial support from the National Natural Science Foundation of China (32272450 and 81703065), the Science Fund for Distinguished Young Scholars of Fujian Province (2023J06020), the Research Fund for Taiwan-Straits Postdoctoral Exchange Program (2018B003), the Natural Science Foundation of Fujian Province (2020I0012, 2020I0010, 2020NZ010011), and the Key Projects of Science and Technology Innovation of Fujian Province (2022G02024).

■ REFERENCES

(1) Swenson, L. S.; Orozco, J. C.; Liu, Y.; Darling, S. B.; Ishaque Khan, M. Novel colloidal materials from functionalized polyoxometalates. *Inorg. Chem. Commun.* **2017**, *84*, 20−23.

(2) Miras, H. N.; Chilas, G. I.; Cronin, L.; Kabanos, T. A. Sulfite Anions as Structure-Directing Templates for the Engineering of Modular Polyoxometalates. *Eur. J. Inorg. Chem.* **2013**, *2013* (10−11), 1620−1630.

(3) Anyushin, A. V.; Kondinski, A.; Parac-Vogt, T. N. Hybrid polyoxometalates as post-functionalization platforms: from fundamentals to emerging applications. *Chem. Soc. Rev.* **2020**, *49* (2), 382−432.

(4) Wang, S.-S.; Yang, G.-Y. Recent Advances in Polyoxometalate-Catalyzed Reactions. *Chem. Rev.* **2015**, *115*, 4893−4962.

(5) Yamase, T. Photo-and electrochromism of polyoxometalates and related materials. *Chem. Rev.* **1998**, *98* (1), 307−326.

(6) Omwoma, S.; Gore, C. T.; Ji, Y.; Hu, C.; Song, Y.-F. Environmentally benign polyoxometalate materials. *Coord. Chem. Rev.* **2015**, *286*, 17−29.

(7) Arab Fashapoyeh, M.; Mirzaei, M.; Eshtiagh-Hosseini, H.; Rajagopal, A.; Lechner, M.; Liu, R.; Streb, C. Photochemical and electrochemical hydrogen evolution reactivity of lanthanide-functionalized polyoxotungstates. *Chem. Commun.* **2018**, *54* (74), 10427−10430.

(8) Bazargan, M.; Mirzaei, M.; Franconetti, A.; Frontera, A. On the preferences of five-membered chelate rings in coordination chemistry: insights from the Cambridge Structural Database and theoretical calculations. *Dalton Trans.* **2019**, *48* (17), 5476−5490.

(9) Babaei Zarch, M.; Mirzaei, M.; Bazargan, M.; Gupta, S. K.; Meyer, F.; Mague, J. T. Single-molecule magnets within polyoxometalate-based frameworks. *Dalton Trans.* **2021**, *50* (42), 15047−15056.

(10) Samaniyan, M.; Mirzaei, M.; Gomila, R. M.; Eshtiagh-Hosseini, H.; Lotfian, N.; Mague, J. T.; Pour, A. N.; Frontera, A. Supramolecular network of a framework material supported by the anion-π linkage of Keggin-type heteropolyoxotungstates: experimental and theoretical insights. *Dalton Trans.* **2021**, *50* (5), 1895−1900.

(11) Mirzaei, M.; Eshtiagh-Hosseini, H.; Lotfian, N.; Salimi, A.; Bauzá, A.; Van Deun, R.; Decadt, R.; Barceló-Oliver, M.; Frontera, A. Syntheses, structures, properties and DFT study of hybrid inorganic-organic architectures constructed from trinuclear lanthanide frameworks and Keggin-type polyoxometalates. *Dalton Trans.* **2014**, *43* (4), 1906−1916.

(12) Mirzaei, M.; Eshtiagh-Hosseini, H.; Alipour, M.; Bauzá, A.; Mague, J. T.; Korabik, M.; Frontera, A. Hydrothermal synthesis, X-ray structure and DFT and magnetic studies of a (H2SiW12O40)2- based one-dimensional linear coordination polymer. *Dalton Trans.* **2015**, *44* (19), 8824−8832.

(13) Najafi, A.; Mirzaei, M.; Mague, J. T. Structural scope of six new layered to pillar-layered hybrid inorganic-organic networks bearing [BW12O40]5- and lanthanoid-cluster; database study toward ligand role in assemblies. *CrystEngComm* **2016**, *18* (35), 6724−6737.

(14) Mirzaei, M.; Eshtiagh-Hosseini, H.; Alipour, M.; Frontera, A. Recent developments in the crystal engineering of diverse coordination modes (0−12) for Keggin-type polyoxometalates in hybrid inorganic-organic architectures. *Coord. Chem. Rev.* **2014**, *275*, 1−18.

(15) Wilke, T. J.; Barteau, M. A. Development of thermodynamic activity coefficients to describe the catalytic performance of supported polyoxometalate catalysts. *J. Catal.* **2020**, *382*, 286−294.

(16) Ali, B.; McCormac, T.; Maccato, C.; Barreca, D.; Carraro, G. Multilayer assemblies of a Cu-phthalocyanine with Dawson type polyoxometalates (POMs) for the electrocatalytic reduction of phosphate. *J. Electroanal. Chem.* **2020**, *858*, 113770.

(17) Jiao, J.; Zuo, J.; Pang, H.; Tan, L.; Chen, T.; Ma, H. A dopamine electrochemical sensor based on Pd-Pt alloy nanoparticles decorated polyoxometalate and multiwalled carbon nanotubes. *J. Electroanal. Chem.* **2018**, *827*, 103−111.

(18) Derakhshanrad, S.; Mirzaei, M.; Streb, C.; Amiri, A.; Ritchie, C. Polyoxometalate-based frameworks as adsorbents for drug of abuse extraction from hair samples. *Inorg. Chem.* **2021**, *60* (3), 1472−1479.

(19) Bazargan, M.; Mirzaei, M.; Amiri, A.; Mague, J. T. Opioid drug detection in hair samples using polyoxometalate-based frameworks. *Inorg. Chem.* **2023**, *62* (1), 56−65.

(20) Bijelic, A.; Rompel, A. Polyoxometalates: more than a phasing tool in protein crystallography. *ChemTexts* **2018**, *4* (3), 10.

(21) Dong, Z.; Yang, Y.; Liu, S.; Lu, J.; Huang, B.; Zhang, Y. HDAC inhibitor PAC-320 induces G2/M cell cycle arrest and apoptosis in human prostate cancer. *Oncotarget* **2017**, *9* (1), 512−523.

(22) Li, X.-H.; Chen, W.-L.; Li, Y.-G.; He, P.; Di, Y.; Wei, M.; Wang, E.-B. Multi-functional rare earth-containing polyoxometalates achieving high-efficiency tumor therapy and visual fluorescence monitoring. *Inorg. Chem. Commun.* **2019**, *104*, 40−47.

(23) Li, Q.; Zhang, H.; qi, Y.; Wang, J.; Li, J.; Niu, J. Antiviral effects of a niobium-substituted heteropolytungstate on hepatitis B virus-transgenic mice. *Drug Dev. Res.* **2019**, *80*, 1062−1070.

(24) Francese, R.; Civra, A.; Rittà, M.; Donalisio, M.; Argenziano, M.; Cavalli, R.; Mougharbel, A. S.; Kortz, U.; Lembo, D. Anti-zika virus activity of polyoxometalates. *Antiviral Res.* **2019**, *163*, 29−33.

(25) Li, L.; Chen, B.; Deng, Y.; Xie, L.; Xing, R.; Wang, L. Inhibitory Effects of Dawson Type Polyoxometalates on Tyrosinase. *Chin. J. Appl. Chem.* **2017**, *34* (1), 83.

(26) Lampl, R.; Breibeck, J.; Gumerova, N. I.; Galanski, M. S.; Rompel, A. Wells-Dawson phosphotungstates as mushroom tyrosinase inhibitors: a speciation study. *Sci. Rep.* **2021**, *11* (1), 19354.

(27) Luong, T.; Govaerts, I.; Robben, J.; Shestakova, P.; Parac-Vogt, T. N. "Polyoxometalates as artificial nucleases: Hydrolytic Cleavage of DNA Promoted by a Highly Negatively Charged ZrIV-Substituted Keggin Polyanion". *Chem. Commun.* **2017**, *53* (3), 617−620.

(28) Luong, T.; Absillis, G.; Shestakova, P.; Parac-Vogt, T. N. Hydrolysis of the RNA model substrate catalyzed by a binuclear ZrIV-

substituted Keggin polyoxometalate. *Dalton Trans.* **2015**, *44*, 15690−15696.
(29) Luong, T. K. N.; Shestakova, P.; Parac-Vogt, T. N. Kinetic studies of phosphoester hydrolysis promoted by a dimeric tetrazirconium (IV) Wells-Dawson polyoxometalate. *Dalton Trans.* **2016**, *45* (30), 12174−12180.
(30) Vanhaecht, S.; Absillis, G.; Parac-Vogt, T. N. Hydrolysis of DNA model substrates catalyzed by metal-substituted Wells-Dawson polyoxometalates. *Dalton Trans.* **2012**, *41* (33), 10028.
(31) Yu, R.; Hou, C.; Liu, A.; Peng, T.; Xia, M.; Wu, X.; Shen, L.; Liu, Y.; li, J.; Yang, F.; et al. Extracellular DNA enhances the adsorption of Sulfobacillus thermosulfidooxidans strain ST on chalcopyrite surface. *Hydrometallurgy* **2018**, *176* (3), 97−103.
(32) Panariello, B. H. D.; Klein, M. I.; Alves, F.; Pavarina, A. C. DNase increases the efficacy of antimicrobial photodynamic therapy on Candida albicans biofilms. *Photodiagn. Photodyn. Ther.* **2019**, *27*, 124−131.
(33) Sher, A. A.; Ashraf, M. A.; Mustafa, B. E.; Raza, M. M. Epidemiological trends of foodborne campylobacter outbreaks in the United States of America, 1998−2016. *Food Microbiol.* **2021**, *97*, 103751.
(34) Nahar, S.; Jeong, H. L.; Kim, Y.; Ha, A. J.-w.; Roy, P. K.; Park, S. H.; Ashrafudoulla, M.; Mizan, M. F. R.; Ha, S.-D. Inhibitory effects of Flavourzyme on biofilm formation, quorum sensing, and virulence genes of foodborne pathogens Salmonella Typhimurium and Escherichia coli. *Food Res. Int.* **2021**, *147*, 110461.
(35) Hu, J.; Tan, S. K.; Lim, M.; Chang, S. H.; Cui, G.; Liu, S.; Narasimhan, K.; New, S. Y.; Wang, X.; Chen, C.; et al. Identification of a Wells-Dawson polyoxometalate-based AP-2γ inhibitor with pro-apoptotic activity. *Biochem. J.* **2018**, *475*, 1965−1977.
(36) Lu, J.; Li, J. L.; Sun, Q.; Jiang, L.; Gu, W.; Liu, X.; Tian, J. L.; Yan, S. P. Synthesis, characterization, and biological activities of two Cu(II) and Zn(II) complexes with one polyquinoline ligand. *Spectrochim. Acta, Part A* **2014**, *130*, 390−396.
(37) Azam, M. W.; Zuberi, A.; Khan, A. U. bolA gene involved in curli amyloids and fimbriae production in E. coli: exploring pathways to inhibit biofilm and amyloid formation. *J. Biol. Res. (Thessaloniki, Greece)* **2020**, *27*, 10.
(38) Sanchez-Torres, V.; Hu, H.; Wood, T. K. GGDEF proteins YeaI, YedQ, and YfiN reduce early biofilm formation and swimming motility in Escherichia coli. *Appl. Microbiol. Biotechnol.* **2011**, *90*, 651−658.
(39) Liu, D.; Tan, H.; Chen, W.; Li, Y.; Wang, E. Resolution of chiral polyoxoanion [P2Mo18O62]6− with histidine. *CrystEngComm* **2010**, *12*, 2044−2046.
(40) Mathew, D.; Sujatha, S. Interactions of porphyrins with DNA: A review focusing recent advances in chemical modifications on porphyrins as artificial nucleases. *J. Inorg. Biochem.* **2021**, *219*, 111434.
(41) Luong, T. K. N.; Absillis, G.; Shestakova, P.; Parac-Vogt, T. N. Solution Speciation of the Dinuclear ZrIV-Substituted Keggin Polyoxometalate [{α-PW11O39Zr(μ-OH)(H2O)}2]8- and Its Reactivity towards DNA-Model Phosphodiester Hydrolysis. *Eur. J. Inorg. Chem.* **2014**, *2014* (31), 5276−5284.
(42) Chen, Z.; Ji, H.; Liu, C.; Bing, W.; Wang, Z.; Qu, X. A multinuclear metal complex based DNase-mimetic artificial enzyme: matrix cleavage for combating bacterial biofilms. *Angew. Chem.* **2016**, *128* (36), 10890−10894.
(43) Lappann, M.; Claus, H.; Van Alen, T.; Harmsen, M.; Elias, J.; Molin, S.; Vogel, U. A dual role of extracellular DNA during biofilm formation of Neisseria meningitidis. *Mol. Microbiol.* **2010**, *75* (6), 1355−1371.
(44) Zhang, S.; Ou, F.; Ning, S.; Cheng, P. Polyoxometalate-based metal-organic frameworks for heterogeneous catalysis. *Inorg. Chem. Front.* **2021**, *8* (7), 1865−1899.
(45) Yokuş, Ö. A.; Kardaş, F.; Akyıldırım, O.; Eren, T.; Atar, N.; Yola, M. L. Sensitive voltammetric sensor based on polyoxometalate/reduced graphene oxide nanomaterial: application to the simultaneous determination of l-tyrosine and l-tryptophan. *Sens. Actuators, B* **2016**, *233*, 47−54.
(46) Green, M.; Li, Y.; Peng, Z.; Chen, X. Dielectric, magnetic, and microwave absorption properties of polyoxometalate-based materials. *J. Magn. Magn. Mater.* **2020**, *497*, 165974.
(47) Hasenknopf, B. Polyoxometalates: introduction to a class of inorganic compounds and their biomedical applications. *Front. Biosci.-Landmark* **2005**, *10* (1−3), 275−287.
(48) Steiner, R. A.; Foreman, D.; Lin, H. X.; Carney, B. K.; Fox, K. M.; Cassimeris, L.; Tanski, J. M.; Tyler, L. A. Synthesis, characterization, crystal structures and biological activity of set of Cu(II) benzothiazole complexes: Artificial nucleases with cytotoxic activities. *J. Inorg. Biochem.* **2014**, *137*, 1−11.
(49) Tomczyk, M. D.; Kuźnik, N.; Walczak, K. Cyclen-based artificial nucleases: Three decades of development (1989−2022). Part a-Hydrolysis of phosphate esters. *Coord. Chem. Rev.* **2023**, *481*, 215047.
(50) Ichikawa, K.; Tarnai, M.; Uddin, M. K.; Nakata, K.; Sato, S. Hydrolysis of natural and artificial phosphoesters using zinc model compound with a histidine-containing pseudopeptide. *J. Inorg. Biochem.* **2002**, *91* (3), 437−450.
(51) Stewart, P. S. Prospects for anti-biofilm pharmaceuticals. *Pharmaceuticals* **2015**, *8* (3), 504−511.
(52) Das, T.; Sehar, S.; Manefield, M. The roles of extracellular DNA in the structural integrity of extracellular polymeric substance and bacterial biofilm development. *Environ. Microbiol. Rep.* **2013**, *5* (6), 778−786.
(53) Okshevsky, M.; Meyer, R. L. The role of extracellular DNA in the establishment, maintenance and perpetuation of bacterial biofilms. *Crit. Rev. Microbiol.* **2013**, *41* (3), 341−352.
(54) Nijland, R.; Hall, M. J.; Burgess, J. G. Dispersal of biofilms by secreted, matrix degrading, bacterial DNase. *PLoS One* **2010**, *5* (12), No. e15668.
(55) Whitchurch, C. B.; Tolker-Nielsen, T.; Ragas, P. C.; Mattick, J. S. Extracellular DNA required for bacterial biofilm formation. *Science* **2002**, *295* (5559), 1487.
(56) Thomas, V. C.; Thurlow, L. R.; Boyle, D.; Hancock, L. E. Regulation of autolysis-dependent extracellular DNA release by Enterococcus faecalis extracellular proteases influences biofilm development. *J. Bacteriol.* **2008**, *190* (16), 5690−5698.
(57) Kaplan, J. B.; LoVetri, K.; Cardona, S. T.; Madhyastha, S.; Sadovskaya, I.; Jabbouri, S.; Izano, E. A. Recombinant human DNase I decreases biofilm and increases antimicrobial susceptibility in staphylococci. *J. Antibiot.* **2012**, *65* (2), 73−77.
(58) Harmsen, M.; Lappann, M.; Knøchel, S.; Molin, S. Role of extracellular DNA during biofilm formation by Listeria monocytogenes. *Appl. Environ. Microbiol.* **2010**, *76* (7), 2271−2279.
(59) Ding, T.; Xuan, X.-T.; Li, J.; Chen, S.; Liu, D.-H.; Ye, X.-Q.; Shi, J.; Xue, S. Disinfection efficacy and mechanism of slightly acidic electrolyzed water on Staphylococcus aureus in pure culture. *Food Control* **2016**, *60*, 505−510.
(60) Pakkulnan, R.; Anutrakunchai, C.; Kanthawong, S.; Taweechaisupapong, S.; Chareonsudjai, P.; Chareonsudjai, S. Extracellular DNA facilitates bacterial adhesion during Burkholderia pseudomallei biofilm formation. *PLoS One* **2019**, *14*, No. e0213288.
(61) Moshynets, O. V.; Baranovskyi, T. P.; Iungin, O. S.; Kysil, N. P.; Metelytsia, L. O.; Pokholenko, I.; Potochilova, V. V.; Potters, G.; Rudnieva, K. L.; Rymar, S. Y.; et al. eDNA Inactivation and Biofilm Inhibition by the PolymericBiocide Polyhexamethylene Guanidine Hydrochloride (PHMG-Cl). *Int. J. Mol. Sci.* **2022**, *23* (2), 731.
(62) Graham, D.; Lathrop, R. C. The synthesis of "optimum" transient response: criteria and standard forms. *Transactions of the American Institute of Electrical Engineers, Part II: Applications and Industry*; Institute of Electrical and Electronics Engineers, 1953; Vol. 72, pp 273−288.
(63) Chinnathambi, S.; Ammam, M. A molecular hybrid polyoxometalate-organometallic moieties and its relevance to supercapacitors in physiological electrolytes. *J. Power Sources* **2015**, *284*, 524−535.

https://doi.org/10.1021/acsomega.3c04790
ACS Omega 2023, 8, 33966−33974